Journal of the Physical Society of Japan **91**, 014704 (2022)
https://doi.org/10.7566/JPSJ.91.014704

Systematic Studies on Magnetism of Divalent 3*d* Transition Metal Ions in Ordered ReO_3-type Fluorides $MZrF_6$ (M = Ti, V, Cr, Mn, Fe, Co, Ni, and Cu)

Hiroaki Ueda, Tatsuki Inamori, Atsushi Taguchi, Chishiro Michioka, and Kazuyoshi Yoshimura

Department of Chemistry, Graduate School of Science, Kyoto University, Sakyo, Kyoto 606-8502, Japan

(Received August 5, 2021; accepted November 22, 2021; published online December 20, 2021)

We have investigated eight magnetic fluorides $MZrF_6$ (M = Ti, V, Cr, Mn, Fe, Co, Ni, and Cu) with ordered ReO_3-type structure, which have face-centered cubic magnetic lattices, using X-ray diffraction, magnetization measurement, and heat capacity measurement. The Ni compound shows an antiferromagnetic order at $T_N = 3.6$ K and a spin-flop transition at 1.2 T. The other compounds show no sign of magnetic ordering down to 2 K. For each compound, temperature dependence of magnetic susceptibility and magnetization process at low temperatures are analyzed using mean-field approximation. It is revealed that the Ti and V compounds have antiferromagnetic interactions and that geometrical frustration suppresses formation of long range magnetic ordering in these compounds. In addition, Ti^{2+} with the fictitious spin state of $J_{eff} = 2$ makes the magnetic system robust against magnetic field.

1. Introduction

Among various inorganic compounds, perovskites ABX_3 have been studied extensively for their interesting physical properties, which include ferroelectricity, superconductivity, colossal magnetoresistance, and so on.[1)] In addition, there are various perovskite-related structures, which makes the system more fascinating. Among them, in perovskites that has ordered cation arrangements known as double perovskites, there are two types of B-site sublattice: layered- and rocksalt-type.[2)] In the latter case, both B and B' sites constitute interpenetrating face-centered cubic (fcc) sublattices.

When nearest neighbor interaction is antiferromagnetic in the face-centered cubic lattice of magnetic ions, the system has geometrical spin frustration. Geometrically frustrated systems have attracted much attention over the past few decades, owing to their exotic ground states, such as spin liquid,[3)] and spin ice states.[4)] Several rocksalt-type magnetic B-site ordered double-perovskites are studied in a view point of spin frustration.[5)]

If A ions are removed from perovskite AMX_3, the system would become MX_3 with ReO_3 structure. Likewise, ordered ReO_3 structure is obtained by removing A ions from rocksalt-type double perovskite A_2BMX_6. Although this structure is hardly found in oxides, many fluorides with chemical formula MBF_6 were reported to have ordered ReO_3 structure.[6)] In most of the cases, B is a non-magnetic tetravalent ion and M is a divalent 3*d* transition metal ion, and M sublattice forms face-centered cubic lattice, which leads possible geometrical frustration. In addition, some of them were reported to exhibit negative thermal expansion.[7,8)] The fluoride system $MZrF_6$ is of particular interest, because it includes compounds with every divalent 3*d* transition metal ion. Hence we can compare magnetic properties of them in the same crystal structure and elucidate the effect of the crystal field, spin–orbit couplings, magnetic interactions and geometrical spin frustration.

In this paper, we report physical properties of ordered ReO_3-type fluorides $MZrF_6$ (M = Ti, V, Cr, Mn, Fe, Co, Ni, and Cu). Most of the compounds behave as weakly interacting spin systems. However, $TiZrF_6$ and $VZrF_6$ have certain amount of antiferromagnetic interactions owing to exchange coupling through t_{2g} orbitals, leading geometrical frustration. And $TiZrF_6$ and $CoZrF_6$ exhibit significant effect of the residual orbital momentum.

2. Experimental Details

Polycrystalline samples of $MZrF_6$ (M = Ti, V, Cr, Mn, Fe, Co, Ni, Cu, and Zn) were synthesized using conventional solid state reactions in Ar atmosphere. As starting materials, we have chosen several substances depending on M. In the case of the Ti and Cr compounds, MF_3, M metal and ZrF_4 were used. For the V compound, VF_3, Zr metal and ZrF_4 were used. Otherwise, MF_2 and ZrF_4 were used. The fluorides MF_2, MF_3, and ZrF_4 were dried or purified before use. In order to compensate sublimed ZrF_4, 5% excess of ZrF_4 was added. Mixtures of starting materials were heated at 650–850 °C for 12 h in sealed copper tubes. Since the samples are very sensitive to water, they were kept in dry Ar atmosphere during synthesis and measurements.

These samples were characterized using a x-ray diffractometer (Miniflex600, Rigaku) with Cu Kα radiation. DC magnetization measurements were performed using a SQUID magnetometer (MPMS, Quantum Design) in Research Center for Low Temperature and Materials Sciences, Kyoto University. Heat capacity measurements were carried out using a two-τ relaxation method (PPMS-14LHS, Quantum Design). The contributions of the lattice heat capacity were evaluated from the heat capacity of $ZnZrF_6$.

3. Results and Discussions

We successfully synthesized eight magnetic fluorides $MZrF_6$ (M = Ti, V, Cr, Mn, Fe, Co, Ni, and Cu) and one non-magnetic $ZnZrF_6$, all of which have ordered ReO_3-type structure. Powder x-ray diffraction showed that crystal structures of all compounds at room temperatures are consistent with previous reports as explained below. For early 3*d* transition metal compounds, the structure is cubic[9,10)] down to low temperatures. Owing to Jahn–Teller effect of Cr^{2+} and Cu^{2+}, $CrZrF_6$ and $CuZrF_6$ are tetragonal at room temperatures.[11,12)] For Ni, the structure at room temperature is rhombohedral.[13)] The structures of the others are cubic at high temperatures, and rhombohedral at low temperatures.[6,13,14)]

Magnetic ions in these compounds form face-centered cubic lattices, although some of them are slightly distorted

especially at low temperatures. To understand magnetic properties of $M\mathrm{ZrF_6}$ with various $3d$ transition metal ions, we measured and analyzed their magnetic susceptibility and magnetization process.

Temperature T dependence of magnetic susceptibility χ of interacting spin system is often described using the Curie–Weiss law, which is written as

$$\chi = \frac{N_\mathrm{A} g^2 \mu_\mathrm{B}^2 S(S+1)}{3k_\mathrm{B}(T-\theta_\mathrm{W})},$$

where N_A is Avogadro's number, g is g-factor, μ_B is Bohr magneton, S is total spin quantum number, k_B is Boltzmann constant, and θ_W is Weiss temperature. Hence, one obtains

$$\chi^{-1}S(S+1) = \frac{3k_\mathrm{B}}{N_\mathrm{A} g^2 \mu_\mathrm{B}^2}(T-\theta_\mathrm{W}).$$

If g equals to the constant value 2, a $\chi^{-1}S(S+1)$–T plot should be a line with a constant slope.

In Fig. 1, T dependences of $\chi^{-1}S(S+1)$ are shown, where S is calculated supposing high spin states. For all compounds, the curves show linear behavior at high temperatures. Except for the Co compound, the curves have almost the same slope as that of the above mentioned theoretical curve with $g = 2$, which is displayed by a black broken line in the figure. This fact indicates that they are well-described as high spin state, which is consistent with previous reports on the V and Cu compounds.[12,15]

For $\mathrm{TiZrF_6}$ and $\mathrm{CoZrF_6}$, the slopes at low temperatures are different from those at high temperatures. These changes in slopes are qualitatively explained in terms of level split owing to spin–orbit couplings, since $\mathrm{Ti^{2+}}$ and $\mathrm{Co^{2+}}$ in an octahedral crystal field have residual orbital momentum. In Fig. 1, colored broken curves show the results of theoretical calculation[16] for non-interacting $\mathrm{Ti^{2+}}$ and $\mathrm{Co^{2+}}$ in octahedral crystal field with spin–orbit couplings $\mathcal{H} = \lambda L \cdot S$, where λ is spin–orbit coupling constant and L is total orbital quantum number. They are written as

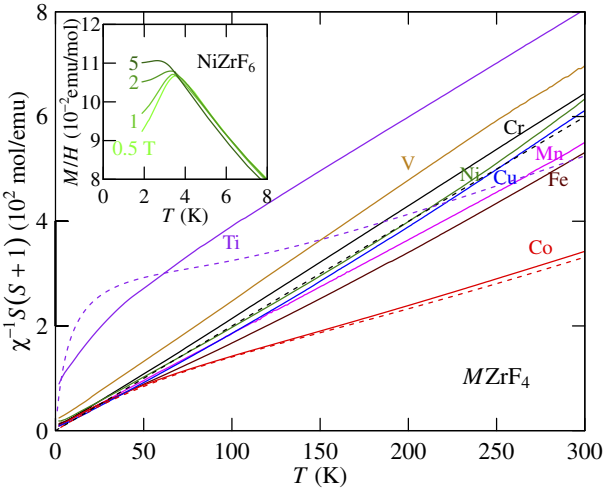

Fig. 1. (Color online) Main panel shows temperature dependence of normalized inverse magnetic susceptibility. Black broken line indicates the theoretical value of $\theta_\mathrm{W} = 0$ K. Colored broken curves are calculated curves obtained by considering spin–orbit couplings for $\mathrm{TiZrF_6}$ and $\mathrm{CoZrF_6}$ using $\lambda = 86$ and -247 K, respectively. For $\mathrm{NiZrF_6}$, data at 5 T is used and ferromagnetic component owing to Ni metal is subtracted. The amount of Ni metal is evaluated to be approximately 0.3%. The other samples are measured at 1 T. The inset shows M/H of $\mathrm{NiZrF_6}$ at low temperatures.

$$\chi(\mathrm{Ti^{2+}}) = \frac{N_\mathrm{A}\mu_\mathrm{B}^2}{3k_\mathrm{B}T} \times \frac{8 + (3x-8)e^{-3x/2}}{x\{2 + e^{-3x/2}\}},$$

$$\chi(\mathrm{Co^{2+}}) = \frac{N_\mathrm{A}\mu_\mathrm{B}^2}{3k_\mathrm{B}T} \times \frac{3\left\{\frac{63x}{20} + \frac{98}{25} + \left(\frac{640x}{225} + \frac{4312}{2025}\right)e^{-\frac{15x}{4}} + \left(\frac{169x}{36} - \frac{490}{81}\right)e^{-6x}\right\}}{x\{3 + 2e^{-\frac{15x}{4}} + e^{-6x}\}},$$

where $x = \lambda/k_\mathrm{B}T$. For $\mathrm{CoZrF_6}$, the difference between the experimental data and this calculation is sufficiently small, suggesting that $\mathrm{Co^{2+}}$ in $\mathrm{CoZrF_6}$ is well-described as a non-interacting spin with spin–orbit couplings. In contrast for $\mathrm{TiZrF_6}$, the experimental data and calculation are substantially different. This fact indicates that $\mathrm{Ti^{2+}}$ ions in $\mathrm{TiZrF_6}$ are not expressed as non-interacting spins, and hence they are highly interacted with each other.

The magnetic susceptibility of $\mathrm{NiZrF_6}$ has a maximum at $T_\mathrm{N} = 3.6$ K as shown in the inset of Fig. 1. This behavior suggests antiferromagnetic ordering below T_N. Below T_N, M/H increases with increasing H, which will be discussed later. The other compounds showed no signs of magnetic ordering down to 2 K, indicating that they are paramagnetic.

To clarify the magnetic states at low temperatures, magnetization process is useful. Magnetization M of a free spin under magnetic field H is expressed as

$$M(H) = gS\mu_\mathrm{B}B_S\left(\frac{gS\mu_\mathrm{B}H}{k_\mathrm{B}T}\right),$$

where $B_S(x)$ is Brillouin function for spin S. In small x region, $B_S(x)$ is approximately equal to $\frac{S+1}{3S}x$. Hence initial slope of a $B_S(x)$–$\frac{S+1}{S}x$ curve is independent of S. In the above formula, M/S–$(S+1)H$ curves have a S-independent slope at constant T at low fields.

In Fig. 2, M/S of $M\mathrm{ZrF_6}$ at 2 K are plotted as a function of $(S+1)\mu_0 H$, where M was measured up to 7 T. For $\mathrm{NiZrF_6}$, which has $S = 1$ spins, the slope of the curve increases approximately at $(S+1)\mu_0 H = 2.5$ T. This fact indicates that a spin-flop transition occurs by applying magnetic field to the magnetically ordered state of $\mathrm{NiZrF_6}$. This is the origin of field dependence of M/H in the inset of Fig. 1. For $\mathrm{TiZrF_6}$ and $\mathrm{VZrF_6}$, M increases almost linearly up to 7 T. For the other compounds, the shapes of the curves are qualitatively similar to Brillouin function. However, the slopes at low fields are smaller than the theoretical value for non-interacting spins, which is indicated by dotted curves in the figure. This fact suggests that they have certain amount of antiferromagnetic interactions.

If spins interact with each other, mean-field approximation gives

$$M = gS\mu_\mathrm{B}B_S\left(\frac{gS\mu_\mathrm{B}H + 2zJSM/g\mu_\mathrm{B}}{k_\mathrm{B}T}\right),$$

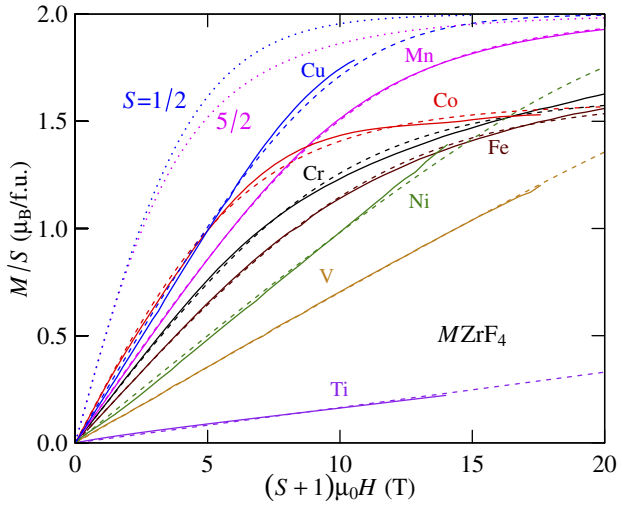

Fig. 2. (Color online) The magnetization processes of MZrF$_6$ at 2 K. Measured curves are shown using solid lines. Theoretical curves for non-interacting $S = 1/2$ and $5/2$ are displayed using dotted curves. Results of mean-field fittings are drawn using broken curves.

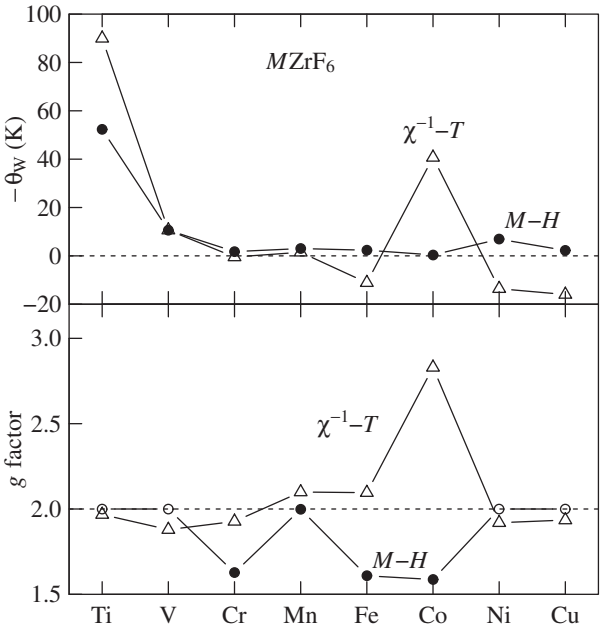

Fig. 3. Weiss temperatures θ_W and g factors evaluated by fitting χ–T data in Fig. 1 (triangle) and M–H data in Fig. 2 (circle). Open circles indicate that g is fixed to 2.

where J is nearest neighbor exchange coupling and z is the number of nearest neighbor spins. Using this formula, we fitted the obtained data, results of which are shown as broken curves in Fig. 2. For Cr, Mn, Fe, and Co compounds, it seems that each M/S tends to saturate. Hence, we deals g as a free parameter in addition to J. For the other compounds, it is difficult to determine g, and g is fixed to 2. Our fittings are consistent with the experimental data as shown in the figure.

We can calculate θ_W from obtained values of J using a formula

$$\theta_W = \frac{2zJS(S+1)}{3k_B}.$$

Values of g and θ_W are also evaluated from fittings of χ^{-1}–T data within high temperature regions where the plots are almost linear. These evaluated values are plotted in Fig. 3.

As shown in the upper panel of Fig. 3, except for TiZrF$_6$ and CoZrF$_6$, absolute values of θ_W for both χ^{-1}–T and M–H fittings are smaller than 20 K, indicating that they have small exchange interactions. As already shown in Fig. 1, the slopes of calculated χ^{-1}–T plot for CoZrF$_6$ differ in low temperature region and in high temperature region owing to mixing of excited states at high temperatures. This makes a large negative value of θ_W at high temperatures, even if there is no antiferromagnetic interactions. The very small difference between the measured χ^{-1}–T curve and the calculation with crystal field and spin–orbit couplings suggests that Co^{2+} in CoZrF$_6$ acts as a nearly free spin. The small value of θ_W evaluated using the M–H curve is consistent with this scenario. In the M–H measurement at 2 K, the spin state of Co^{2+} remains the ground state even under magnetic field of 7 T and the effect of excited state is negligible. Hence, the value obtained using M–H data is more reliable than that using χ^{-1}–T data. For TiZrF$_6$, both θ_W values evaluated using two kinds of fitting are negative, indicating that Ti^{2+} ions are antiferromagnetically coupled. Absolute value of θ_W evaluated using χ^{-1}–T fitting is larger than that using the M–H curve. This is seemingly because that of χ^{-1}–T fitting is enhanced by residual orbital momentum of Ti^{2+}. In addition, the values of θ_W evaluated using both kinds of fitting for VZrF$_6$ are almost the same negative value of −10 K, indicating small antiferromagnetic interactions. Electron configurations of Ti^{2+} and V^{2+} are t_{2g}^2 and t_{2g}^3, respectively. In the crystal structure, nearest neighboring transition metal ions interact through their t_{2g} orbitals. Although the distance between two magnetic ions is relatively large, kinetic exchange interactions through t_{2g} orbitals are likely to be the origin of antiferromagnetic interactions in TiZrF$_6$ and VZrF$_6$. Since, they show no sign of magnetic ordering down to 2 K, the frustration indices $f = |\theta_W|/T_N$ of Ti and V compounds are $f > 27$ and 5, respectively.

The lower panel of Fig. 3 shows that all the g values evaluated using χ^{-1}–T plots are approximately 2, except for the Co compound. The discrepancy from 2 in the Co compound is due to spin–orbit coupling. In contrast, g values evaluated using M–H plots of Cr, Fe, and Co compounds are substantially smaller than 2, which is consistent with the fact that M of these three compounds tend to saturate below $2S\mu_B$. This is possibly because their magnetic ions have degenerated spin states and residual orbital moments.

Specific heat measurements under magnetic field were conducted to clarify the magnetic state of CoZrF$_6$. In the upper panel of Fig. 4, magnetic specific heat C_m divided by T is plotted as a function of T under each magnetic field. Under each magnetic field, a Schottky-type peak is observed, and the position of the peak shifts to higher temperature by applying magnetic field. These curves are well-fitted using the formula of two level Schottky model

$$C = R\left(\frac{\Delta}{k_B T}\right)^2 \frac{e^{\Delta/k_B T}}{(1+e^{\Delta/k_B T})^2},$$

where R is the gas constant, and Δ is gap energy. Obtained values of Δ are plotted as a function of magnetic field in the inset of Fig. 4. The magnetic ground state of free Co^{2+} in a octahedral crystal field is described using fictitious spin

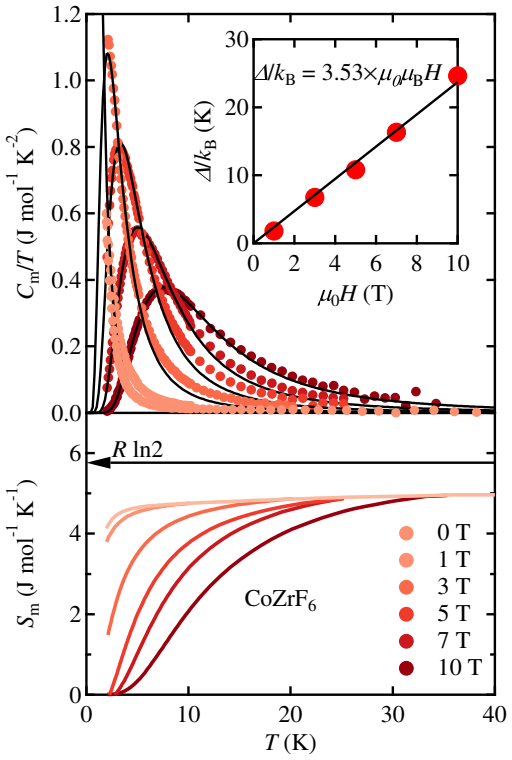

Fig. 4. (Color online) Upper panel shows temperature dependence of magnetic heat capacity divided by temperature, C_m/T, of $CoZrF_6$. Lattice contributions have been already subtracted. The broad peaks imply Schottky-type heat capacity. Black solid lines are Schottky-type fitting curves for each C_m/T except for $H = 0$ T and the gap energy Δ is plotted in the inset. The lower panel shows magnetic entropy. The horizontal solid line indicates $S_m = R \ln 2$, which is expected for $S = \frac{1}{2}$.

$J_{eff} = 1/2$, which is formed owing to spin–orbit couplings between spin and residual orbital momentum. The Zeeman splitting of $J_{eff} = 1/2$ state under magnetic field equals to $g\mu_0\mu_B H$, which is the origin of Schottky-type T-dependence of C. From the linear fitting of Δ as a function of H, we obtained $g = 3.53$ as shown in the inset of Fig. 4. Hence, magnetic moment is $gJ_{eff} = 1.76$. This value is approximately 25% smaller than the value of $gS = 2.4$ for $S = 3/2$, which is evaluated using the M–H fitting. In the fictitious spin model under slightly distorted octahedral crystal field, powder averaged g-value is evaluated to be in the range of 2 to 2.2. This model is consistent with our experimental values, which are smaller than the spin only value of 3. The smaller value evaluated from Schottky-type fittings is likely due to anisotropy of g factor.

The lower panel of Fig. 4 shows magnetic entropy, which is obtained by integrating C_m/T. At low temperatures, S decreases with applying magnetic field owing to the increasement of Zeeman splitting. The magnetic entropy under each field is close to $R \ln 2$ at 40 K rather than $R \ln 4$. Magnetic entropy also indicates that Co^{2+} is not in a spin state of $S = 3/2$ but in a fictitious spin state of $J_{eff} = 1/2$.

In contrast, specific heat of $TiZrF_6$ is robust against magnetic field. As shown in Fig. 5, temperature dependence of C_m/T is similar to a Schottky behavior, in which the broad peak is approximately at 8.1 K. However, the behavior under 14 T is almost the same as that under 0 T. This fact suggests that the magnetic state of $TiZrF_6$ is almost independent of applied magnetic field. This is possibly because of strong

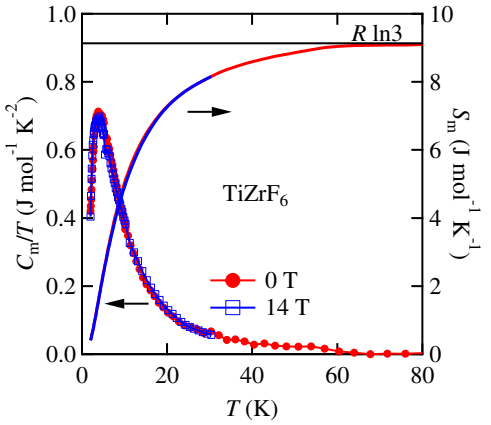

Fig. 5. (Color online) Temperature dependence of magnetic heat capacity divided by temperature, C_m/T of $TiZrF_6$. Lattice contribution have been already subtracted. Filled circles and open squares denote data measured at 0 and 14 T, respectively. Solid lines denote magnetic entropy S_m. The horizontal solid line indicates $S_m = R \ln 3$, which is expected for $S = 1$.

exchange field owing to antiferromagnetic interaction, which is indicated by the analysis of χ–T curve. The Schottky-like T-dependence is thought to be not due to existence of two energy levels but due to development of short-range magnetic orderings driven by nearest neighbor antiferromagnetic interactions.

With increasing temperature, magnetic entropy gradually increases, and reaches $R \ln 3$ approximately at 60 K, which is close to $|\theta_W|$ obtained from the M–H curve. However, it is not natural that all magnetic entropy of $S = 1$ is released at $|\theta_W|$. Owing to the residual orbital momentum in octahedral crystal field, the ground state of Ti^{2+} ions is in a fictitious spin state of $J_{eff} = 2$, which has entropy of $R \ln 5$. It is natural to think that 68% of magnetic entropy of $J_{eff} = 2$ is released at $|\theta_W|$. Above experimental observation suggests that Ti^{2+} ions of $TiZrF_6$ is in a $J_{eff} = 2$ state rather than an $S = 1$ state.

In summary, we have studied magnetic properties of $MZrF_6$ (M = Ti, V, Cr, Mn, Fe, Co, Ni, and Cu), all of which have ordered ReO_3-type structure. The Ni compound shows an antiferromagnetic order at $T_N = 3.6$ K and the other compounds show no sign of magnetic ordering down to 2 K. Analysis using mean-field approximation revealed that the Ti and V compounds have antiferromagnetic interactions through t_{2g} electrons and that the other compounds have small magnetic interactions. In addition, geometrical spin frustration has large effect on physical properties of $TiZrF_6$. Although magnetic susceptibility of the Co compound gives negative Weiss temperature, this is not due to the presence of antiferromagnetic interaction but due to the formation of fictitious spin state of $J_{eff} = 1/2$.

Acknowledgments This work was supported by a Grant-in-Aid for Scientific Research (B) Grant Number 18H01179 from the Japan Society for the Promotion of Science.

1) A. S. Bhalla, R. Guo, and R. Roy, Mater. Res. Innovations **4**, 3 (2000).
2) M. T. Anderson, K. B. Greenwood, G. A. Taylor, and K. R. Poeppelmeier, Prog. Solid State Chem. **22**, 197 (1993).
3) L. Savary and L. Balents, Rep. Prog. Phys. **80**, 016502 (2017).
4) S. T. Bramwell and M. J. P. Gingras, Science **294**, 1495 (2001).
5) T. Aharen, J. E. Greedan, C. A. Bridges, A. A. Aczel, J. Rodriguez, G.

MacDougall, G. M. Luke, T. Imai, V. K. Michaelis, S. Kroeker, H. Zhou, C. R. Wiebe, and L. M. D. Cranswick, Phys. Rev. B **81**, 224409 (2010).
6) V. D. Reinen and F. Steffens, Z. Anorg. Allg. Chem. **441**, 63 (1978).
7) J. C. Hancock, K. W. Chapman, G. J. Halder, C. R. Morelock, B. S. Kaplan, L. C. Gallington, A. Bongiorno, C. Han, S. Zhou, and A. P. Wilkinson, Chem. Mater. **27**, 3912 (2015).
8) J. Xu, L. Hu, Y. Song, F. Han, Y. Qiao, J. Deng, J. Chen, and X. Xing, J. Am. Ceram. Soc. **100**, 5385 (2017).
9) M. Kraus, M. Müller, R. Fischer, R. Schmidt, D. Koller, and B. G. Müller, J. Fluorine Chem. **101**, 165 (2000).
10) R. Schmidt, M. Kraus, and B. G. Müller, Z. Anorg. Allg. Chem. **627**, 2344 (2001).
11) H. Mayer, D. Reinen, and G. Heger, J. Solid State Chem. **50**, 213 (1983).
12) C. Friebel, J. Pebler, F. Steffens, M. Weber, and D. Reinen, J. Solid State Chem. **46**, 253 (1983).
13) B. Garrard and B. Wanklyn, J. Cryst. Growth **47**, 159 (1979).
14) V. Rodriguez, M. Couzi, A. Tressaud, J. Grannec, J. P. Chaminade, and J. L. Soubeyroux, J. Phys.: Condens. Matter **2**, 7373 (1990).
15) T. Le Mercier, J. Chassaing, D. Bizot, and M. Quarton, Mater. Res. Bull. **27**, 259 (1992).
16) O. Kahn, *Molecular Magnetism* (Wiley-VCH, Weinheim, 1993).